Selenium isotopes as tracers of a late volatile contribution to Earth from the outer Solar System

María Isabel Varas-Reus [1]*, Stephan König[1], Aierken Yierpan [1], Jean-Pierre Lorand[2] and Ronny Schoenberg [1]

The origin of Earth's volatiles has been attributed to a late addition of meteoritic material after core–mantle differentiation. The nature and consequences of this 'late veneer' are debated, but may be traced by isotopes of the highly siderophile, or iron-loving, and volatile element selenium. Here we present high-precision selenium isotope data for mantle peridotites, from double spike and hydride-generation multicollector inductively coupled plasma mass spectrometry. These data indicate that the selenium isotopic composition of peridotites is unaffected by petrological processes, such as melt depletion and melt-rock reaction, and thus a narrow range is preserved that is representative of the silicate Earth. We show that selenium isotopes record a signature of late accretion after core formation and that this signature overlaps only with that of the CI-type carbonaceous chondrites. We conclude that these isotopic constraints indicate the late veneer originated from the outer Solar System and was of lower mass than previously estimated. Thus, we suggest a late and highly concentrated delivery of volatiles enabled Earth to become habitable.

Volatiles are key in the development of Earth into a habitable planet, but their origin remains highly debated[1–5]. A 'late veneer' of chondrite-like material added to the bulk silicate Earth (BSE) after core formation had ceased, has been argued to be the most plausible source of Earth's volatiles[4,5]. This late veneer was originally proposed to account for the abundances of highly siderophile elements (HSEs) in the Earth's mantle[6–8]. The model was then extended to volatiles S, Se and Te (refs [5,6]), as all these elements display broadly chondritic relative and absolute abundances in the Earth's mantle higher than experimentally predicted from metal/silicate partition coefficients and core–mantle differentiation models[9–11]. Despite the potential role of the late veneer in Earth's volatile evolution[3–5], its nature remains controversial. Based on Re–Os isotope systematics, the late veneer composition was similar to that of ordinary or enstatite chondrites[12,13], whereas the distinct nucleosynthetic Ru isotope anomalies between the Earth's mantle and known chondrites rule out an outer Solar System origin for the late veneer[2]. These isotope constraints discard carbonaceous chondrites, which, based on their distinct isotope anomalies, are considered to have formed in the outer Solar System[14,15], as the source material of the late veneer. In contrast, the broadly chondritic S, Se and Te ratios in fertile peridotites suggest that the late veneer was volatile-rich and consisted mostly of carbonaceous chondrite-like materials[5]. However, the use of S, Se and Te ratios in mantle peridotites to trace the composition of the late veneer has been significantly weakened as their relative abundances may not represent a primitive feature of the BSE[16,17].

Unravelling the link between the late veneer and Earth's volatiles has proved challenging, mainly because it is difficult to establish precise and accurate volatile isotopic and compositional signatures in the BSE and to attribute them to a clear post-planetary core formation origin[1,5,18]. Here we use Se stable isotopes that, due to their unique properties, can clearly overcome these limitations. Se and Te are both volatile and behave like HSEs at core formation conditions[9], and as HSEs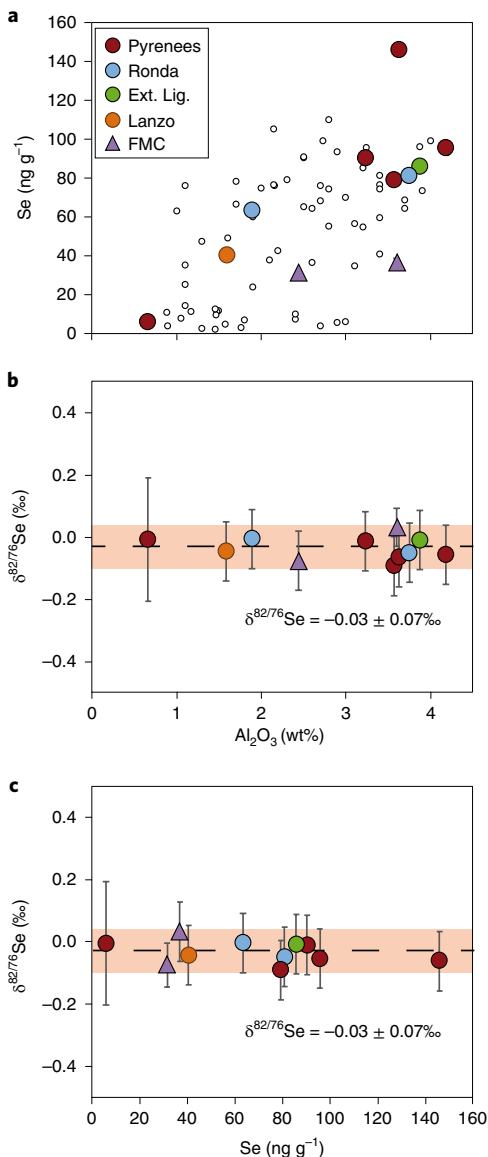 they were almost entirely scavenged from the mantle during core segregation. This Se–Te depleted mantle provides an ideal background for the late veneer to leave a diagnostic signature of these elements. In addition, a recent high-precision study reported distinguishable Se isotope compositions between different classes of chondrites[19]. Altogether, this shows that Se isotopes may potentially be a strong diagnostic tool to identify the type of chondrite representative of the late veneer composition that left its mark in the BSE, provided that such a BSE signature can be established. However, a Se isotope composition of the BSE with similar high-precision to that of chondrites[19] is still missing. We here address this issue by investigating the Se isotope composition of mantle peridotites with a high-precision analytical technique.

Se isotope signature of the BSE inferred from peridotites

For this study, we selected a set of representative mantle peridotites that range in age from mid-Proterozoic to late Palaeozoic and are from different geological settings and localities, which include nine samples from orogenic and transitional peridotite massifs (Ronda, Pyrenees, Lanzo and External Ligurides) and two xenoliths from the French Massif Central (Supplementary Table 1). Samples were analysed for Se isotopes on a multicollector inductively coupled plasma mass spectrometer (MC–ICP–MS) at the University of Tuebingen using a double spike and methane-boosted hydride generation technique[20,21] (Methods). Data are reported in $\delta^{82/76}$Se notation (Supplementary Table 2), that is, the per mil (‰) variation of ^{82}Se/^{76}Se relative to the reference material NIST SRM 3149.
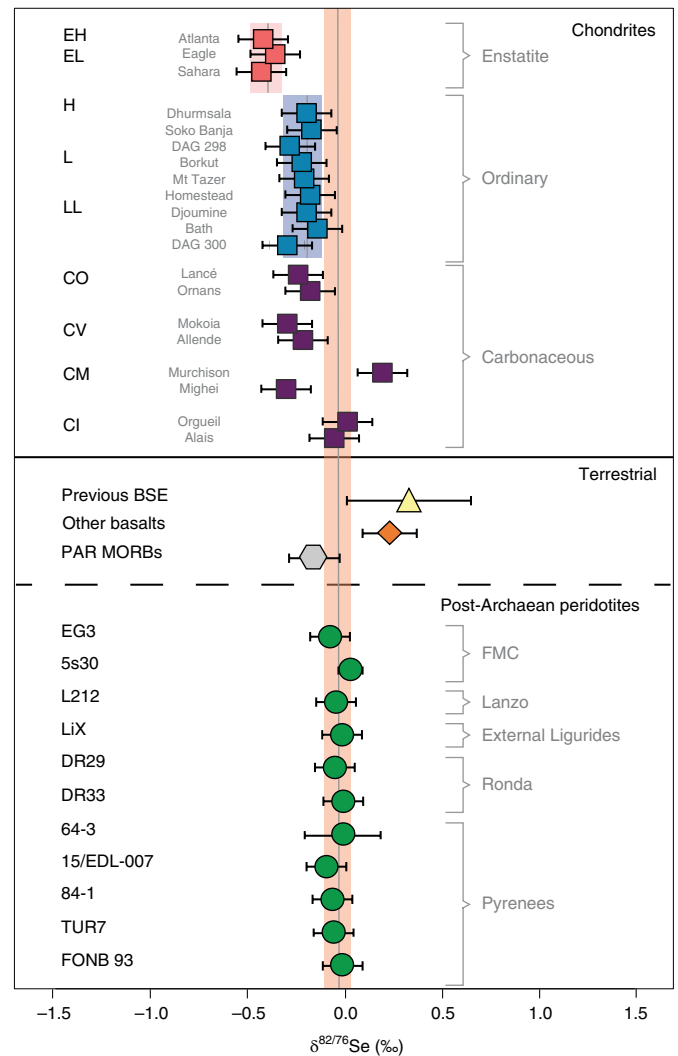
The selected samples range from a refractory harzburgite ($Al_2O_3 \approx 0.7$ wt%, $Se \approx 6$ ng g^{-1}) to a highly fertile lherzolite ($Al_2O_3 \approx 4.2$ wt%, $Se \approx 100$ ng g^{-1}). This sample set displays an apparently positive correlation between the Al_2O_3 and Se contents and encompasses the entire spectrum reported in the literature for peridotites in the Al_2O_3 versus Se space (Fig. 1a). Both depletion and metasomatic re-enrichment processes can account for trends between Al_2O_3 and Se concentrations in peridotites; even refertilization and overprint of the HSEs (including Se and Te) of originally

Fig. 1 | Se and Al₂O₃ contents and Se isotope data of mantle peridotites.
a–c, Se versus Al_2O_3 (**a**), $\delta^{82/76}Se$ versus Al_2O_3 (**b**) and $\delta^{82/76}Se$ versus Se of post-Archaean peridotites (**c**). Circles represent orogenic and transitional peridotites and triangles mantle xenoliths. Small circles in **a** correspond to previously published peridotite data[5,16]. The 1 s.d. uncertainties of the concentrations are similar to or smaller than the symbol size, whereas the error bars in **b** and **c** indicate 2 s.d. uncertainties of more than two combined measurements. If not available, the analytical uncertainty obtained for repeated analyses of peridotites is reported (±0.10‰, 2 s.d.) (Methods). The shaded field represents the 2 s.d. of the mean of peridotites as discussed in the text. Ext. Lig., External Ligurides; FMC, French Massif Central.

Fig. 2 | Se isotope data for terrestrial and meteorite samples. $\delta^{82/76}Se$ values of the analysed peridotites (for simplicity, all as circles) together with published data for terrestrial melts, which include basalts from a variety of geodynamic settings (diamond symbol)[20] and mid-ocean ridge basalts from the Pacific–Antarctic ridge (PAR MORBs)[17]. Also shown are published data for the BSE[27] (2 s.d. analytical precision; average based on iron meteorites and igneous reference materials) and meteorites[19]. The 2 s.d. analytical precision for individual chondrites is 0.13‰ and weathered chondrites are not shown, as they are associated with isotopic fractionation[19]. Literature data[27] are converted into $\delta^{82/76}Se$ following Carignan and Wen[42]. Error bars for peridotites indicate 2 s.d. uncertainties of more than two combined measurements. If not available, the analytical uncertainty obtained for repeated analyses of peridotites is reported (±0.10‰, 2 s.d.) (Methods). Shaded bars indicate the mean $\delta^{82/76}Se$ values of the BSE and of enstatite and ordinary chondrites (±2 s.d.)[19].

refractory peridotite protoliths, have been reported[16,22–25]. However, regardless of these complex mantle processes that might have affected the Se budget of mantle peridotites, they do not produce a Se isotopic variation in peridotites, as shown by their homogeneous $\delta^{82/76}Se$ values ($\delta^{82/76}Se(‰) = [(^{82}Se/^{76}Se)_{sample}/(^{82}Se/^{76}Se)_{std} - 1] \times 1{,}000$, Supplementary Table 2), which have a mean of $-0.03 \pm 0.07‰$ (2 s.d. of the mean, $n = 11$, Fig. 1b,c), and the lack of any correlation with petrogenetic indicators of melt depletion and/or metasomatism such as Al_2O_3 (Fig. 1b) or Pd/Ir ratios (Supplementary Information). This is the most limited Se isotope range reported for

a suite of mantle rocks of different ages and different geological settings, and it is independent of their Se content (Fig. 1c). Compared to peridotites, basaltic lavas from worldwide locations have heavier Se isotope values ($0.23 \pm 0.14‰$, 2 s.d. of the mean, $n = 4$, Fig. 2)[20], whereas Pacific–Antarctic ridge mid-ocean ridge basalts are much lighter ($-0.16 \pm 0.13‰$, 2 s.d. of the mean, $n = 27$, Fig. 2)[17]. This Se isotope variability among basaltic melts might reflect additional processes[26], which emphasizes that selected peridotites, with their range of ages, may indeed represent the most robust estimate of the BSE Se isotope signature.

Implications for the nature of the late veneer

The proposed average BSE Se isotope composition ($-0.03 \pm 0.07‰$, 2 s.d. of the mean) has a remarkably narrow range compared to previous estimates ($0.33 \pm 0.32‰$, 2 s.d. analytical precision, $n = 10$, Fig. 2)[27]. This allows us to resolve a Se isotopic variability between the BSE and different classes of chondrites (reported with 2 s.d. of the mean obtained following replicate measurements, n = number of chondrite subtypes analysed, Fig. 2)[19]. The significantly lighter and homogeneous $\delta^{82/76}$Se value of enstatite chondrites ($-0.40 \pm 0.08‰$, $n = 3$) compared to that of the BSE discard these meteorites as the source of the Se isotopic signature of the BSE (Fig. 2). Ordinary chondrites ($-0.21 \pm 0.10‰$, $n = 9$) and CO ($-0.20 \pm 0.07‰$, $n = 2$) and CV ($-0.24 \pm 0.10‰$, $n = 2$) carbonaceous chondrites can also be discarded as their mean $\delta^{82/76}$Se values are indistinguishable from each other[19], but are statistically significantly different than that of the BSE (Student's t-test, two-tail P value <0.0001, Fig. 2). The CM carbonaceous chondrites Murchison ($0.20 \pm 0.13‰$) and Mighei ($-0.30 \pm 0.10‰$) have substantially different positive and negative $\delta^{82/76}$Se values, respectively, plotting on both sides of the BSE (Fig. 2). These distinct $\delta^{82/76}$Se values suggest that a mixture of these two chondrites could result in a Se isotope signature that overlaps with that of the BSE. However, the possible proportional contributions of Mighei and Murchison chondrite-like material fall within a limited range ($f = 0.69 \pm 0.2$, where f denotes the proportion of source 1 in the mixture, Supplementary Information). Although CM chondrites cannot be refuted as the source of Se in the BSE, and other potential mixtures that involve CI chondrite-like material as the main source can be envisaged, the remarkable overlap of exclusively CI carbonaceous chondrites (mean $\delta^{82/76}$Se value of $-0.02 \pm 0.12‰$, $n = 2$) with the BSE (Fig. 2) advocates for a simpler and straightforward scenario in which CI chondrites alone can account for the BSE Se isotope composition.

We conclude, based on the highly siderophile behaviour of Se at core forming conditions and core–mantle differentiation that left the mantle almost completely devoid of Se[9], that the main and most likely source of Se in the BSE was a CI chondrite-like late veneer. This finding has striking implications for the mass of the late veneer and the amount of volatiles delivered by it. CI chondrites have the highest concentrations of volatiles among carbonaceous chondrites[28], which implies that, compared to previous estimates calculated based on a bulk chondritic composition[8], the mass of the late veneer would be lower. Unlike the estimated BSE Se–Te abundances that are controversial[5,16,17], the S budget is known to retain an imprint acquired during core segregation[29] and thus it has been well constrained in the mantle before and after the late veneer[30,31]. Following a simple batch mixing calculation that assumes ~40% of S is in the pre-late veneer mantle[30] and a BSE S content of $200 \pm 40\,\mu g\,g^{-1}$ (ref. [31]), our mass balance calculations indicate that the total added material to the BSE by a CI chondrite-like late veneer would have been ~0.15 ± 0.03% of the Earth's mass (Supplementary Information). This estimate is significantly lower than the ~0.5% calculated based on mantle HSE abundances and a late veneer of bulk chondritic material[8]. Even considering a CM chondrite-like late veneer (~0.26 ± 0.05% of the Earth's mass, Supplementary Information), the estimated mass would remain lower. This dichotomy could be reconciled if HSE partition coefficients during mantle–core differentiation conditions are lower than those previously reported[10], as proposed for some HSEs[10,11,32]. Other more complex scenarios that involve mixtures of CI chondrite-like material with a minor proportion of other carbonaceous or even ordinary chondrites could account for a Se isotope signature similar to that of the BSE. However, any of these potential mixtures will require more than 85% of CI chondrite-like material, with a similarly low-mass late veneer (Supplementary Information). Alternatively, it has been suggested that the late veneer involved a mixture of ~80% carbonaceous chondrite-like material with ~20%

of a chemically evolved metal component derived from the core of a planetary embryo, similar in composition to iron meteorites[33]. Recent Ru isotopic data, however, challenge this scenario and preclude that a chemically evolved metal component contributed significantly to the late veneer[2,34]. Independent of the likelihood of such intricate scenarios, the Se isotope approach clearly indicates that carbonaceous chondrites dominated the volatile late-accreted material.

These new Se isotope data are also at odds with the Re–Os isotope systematics that support an enstatite- or ordinary-chondrite-like late veneer[12,13] and with Ru isotope anomalies that infer an inner Solar System origin for the late veneer[2]. The mass-dependent Ru isotope systematics, however, show no resolvable differences between the BSE and chondrites[34], similar to the information conveyed by Pt and Pd stable isotopes[35,36], and thus mass-dependent Ru isotope systematics cannot constrain which type of chondrite-like material dominated the late veneer. Furthermore, studies regarding the potential Ru isotope anomalies in the pre-late veneer mantle are currently underway to further assess the timing of the volatile element accretion[37]. Regarding Os isotopes, Meisel et al.[13] and, more recently, Day et al.[38] reported indistinguishable ^{187}Os/^{188}Os ratios for the BSE by extrapolating the correlations between a melt depletion indicator (Al_2O_3) and the ^{187}Os/^{188}Os ratios from worldwide peridotites. Their estimated BSE values (at 4–4.5 wt% Al_2O_3) are most similar to the average of the ordinary and enstatite chondrites, but are higher than those of carbonaceous chondrites[13,38] and any potential mixture that involves a large contribution from the latter (Supplementary Information). The Os isotopic composition of the BSE[13,38] can be reconciled with a late veneer composed of a mixture of carbonaceous chondrites with a chemically evolved metal component, as previously suggested[33]. However, as stated above, this scenario is not supported by mass-dependent and -independent Ru isotopic data[2,34]. In any case, the narrow range of the BSE Se isotope signature reported here clearly overlaps only with that of CI chondrites (Fig. 2). Hence, this is unambiguous evidence that, at least for volatiles, the late veneer comprised objects sourced from the outer Solar System.

Late volatile contribution from the outer Solar System

Given a CI chondrite-like late veneer and a 40% S content in the pre-late veneer mantle[30], the Se content of the BSE ($47 \pm 10\,ng\,g^{-1}$ based on the new estimated late veneer mass, Supplementary Information) would have been delivered along with other volatiles[4,5], but to a different extent. For S it is known that, due to its moderately siderophile nature, ~60% of the total S in the BSE was delivered after core formation[30]. Similar to Se, the highly siderophile behaviour of Te during mantle–core differentiation supports a late veneer as its main source[5,9] and yields a Te BSE abundance of $5 \pm 1\,ng\,g^{-1}$ (Supplementary Information). This heterogeneous contribution of volatiles can also be extended to essential components for life, such as water, carbon and nitrogen. On the basis of recent estimates of their BSE values, a CI chondrite-like late veneer would have delivered ~20–60% of water, from ~50% to even more than 120% of carbon and an excess of nitrogen to the BSE. These estimates remain fairly similar if we consider a CM chondrite-like late veneer, as these chondrites are also volatile-rich materials and would yield Se and Te abundances closer to those of highly fertile lherzolites[5,16,22] (Supplementary Information). Our results imply that a percentage of water and probably carbon must have been delivered during the main stages of planetary accretion, in agreement with previous studies[1,3,39,40]. The excess abundance of nitrogen can be reconciled with considerable atmospheric loss[41] after the late veneer. Yet overall, although the proportion of volatiles delivered depends on their background mantle concentrations, our data also indicate that the late veneer contributed significantly to the Earth's volatile budget.

Online content

Any methods, additional references, Nature Research reporting summaries, source data, statements of code and data availability and associated accession codes are available at https://doi.org/10.1038/s41561-019-0414-7.

References

1. Marty, B. The origins and concentrations of water, carbon, nitrogen and noble gases on Earth. *Earth Planet. Sci. Lett.* **313–314**, 56–66 (2012).
2. Fischer-Gödde, M. & Kleine, T. Ruthenium isotopic evidence for an inner Solar System origin of the late veneer. *Nature* **541**, 525–527 (2017).
3. Morbidelli, A. et al. Source regions and timescales for the delivery of water to the Earth. *Meteorit. Planet. Sci.* **35**, 1309–1320 (2000).
4. Albarède, F. Volatile accretion history of the terrestrial planets and dynamic implications. *Nature* **461**, 1227–1233 (2009).
5. Wang, Z. & Becker, H. Ratios of S, Se and Te in the silicate Earth require a volatile-rich late veneer. *Nature* **499**, 328–331 (2013).
6. McDonough, W. F. & Sun, S-s. The composition of the Earth. *Chem. Geol.* **120**, 223–253 (1995).
7. Chou, C.-L. Fractionation of siderophile elements in the Earth's upper mantle. *Lunar Planet. Sci. Conf. Proc.* **IX**, 219–230 (1978).
8. Walker, R. J. Highly siderophile elements in the Earth, Moon and Mars: update and implications for planetary accretion and differentiation. *Chem. Erde Geochem.* **69**, 101–125 (2009).
9. Rose-Weston, L., Brenan, J. M., Fei, Y., Secco, R. A. & Frost, D. J. Effect of pressure, temperature, and oxygen fugacity on the metal–silicate partitioning of Te, Se, and S: implications for Earth differentiation. *Geochim. Cosmochim. Acta* **73**, 4598–4615 (2009).
10. Mann, U., Frost, D. J., Rubie, D. C., Becker, H. & Audétat, A. Partitioning of Ru, Rh, Pd, Re, Ir and Pt between liquid metal and silicate at high pressures and high temperatures—implications for the origin of highly siderophile element concentrations in the Earth's mantle. *Geochim. Cosmochim. Acta* **84**, 593–613 (2012).
11. Brenan, J. M. & McDonough, W. F. Core formation and metal–silicate fractionation of osmium and iridium from gold. *Nat. Geosci.* **2**, 798–801 (2009).
12. Walker, R. J. et al. Comparative ¹⁸⁷Re–¹⁸⁷Os systematics of chondrites: implications regarding early Solar System processes. *Geochim. Cosmochim. Acta* **66**, 4187–4201 (2002).
13. Meisel, T., Walker, R. J., Irving, A. J. & Lorand, J.-P. Osmium isotopic compositions of mantle xenoliths: a global perspective. *Geochim. Cosmochim. Acta* **65**, 1311–1323 (2001).
14. Warren, P. H. Stable-isotopic anomalies and the accretionary assemblage of the Earth and Mars: a subordinate role for carbonaceous chondrites. *Earth Planet. Sci. Lett.* **311**, 93–100 (2011).
15. Kruijer, T. S., Burkhardt, C., Budde, G. & Kleine, T. Age of Jupiter inferred from the distinct genetics and formation times of meteorites. *Proc. Natl Acad. Sci. USA* **114**, 6712–6716 (2017).
16. König, S., Lorand, J.-P., Luguet, A. & Pearson, D. G. A non-primitive origin of near-chondritic S–Se–Te ratios in mantle peridotites; implications for the Earth's late accretionary history. *Earth Planet. Sci. Lett.* **385**, 110–121 (2014).
17. Yierpan, A., König, S., Labidi, J. & Schoenberg, R. Selenium isotope and S–Se–Te elemental systematics along the Pacific–Antarctic ridge: role of mantle processes. *Geochim. Cosmochim. Acta* **249**, 199–224 (2019).
18. Alexander, C. M. O. D. et al. The provenances of asteroids, and their contributions to the volatile inventories of the terrestrial planets. *Science* **337**, 721–723 (2012).
19. Labidi, J., König, S., Kurzawa, T., Yierpan, A. & Schoenberg, R. The selenium isotopic variations in chondrites are mass-dependent; implications for sulfide formation in the early Solar System. *Earth Planet. Sci. Lett.* **481**, 212–222 (2018).
20. Yierpan, A. et al. Chemical sample processing for combined selenium isotope and selenium–tellurium elemental investigation of the Earth's igneous reservoirs. *Geochem. Geophys. Geosyst.* **19**, 516–533 (2018).
21. Kurzawa, T., König, S., Labidi, J., Yierpan, A. & Schoenberg, R. A method for Se isotope analysis of low ng-level geological samples via double spike and hydride generation MC–ICP–MS. *Chem. Geol.* **466**, 219–228 (2017).
22. Lorand, J.-P. & Alard, O. Determination of selenium and tellurium concentrations in Pyrenean peridotites (Ariege, France): new insight into S/Se/Te systematics of the upper in mantle samples. *Chem. Geol.* **278**, 120–130 (2010).
23. Lorand, J.-P. & Alard, O. Platinum-group element abundances in the upper mantle: new constraints from in situ and whole-rock analyses of Massif Central xenoliths (France). *Geochim. Cosmochim. Acta* **65**, 2789–2806 (2001).
24. Lorand, J.-P., Alard, O., Luguet, A. & Keays, R. R. Sulfur and selenium systematics of the subcontinental lithospheric mantle: inferences from the Massif Central xenolith suite (France). *Geochim. Cosmochim. Acta* **67**, 4137–4151 (2003).
25. Harvey, J., König, S. & Luguet, A. The effects of melt depletion and metasomatism on highly siderophile and strongly chalcophile elements: S–Se–Te–Re–PGE systematics of peridotite xenoliths from Kilbourne Hole, New Mexico. *Geochim. Cosmochim. Acta* **166**, 210–233 (2015).
26. Kurzawa, T., König, S.J. C., Yierpan, A. & Schoenberg, R. The role of subduction recycling on the selenium isotope signature of the mantle: constraints from Mariana arc lavas. *Chem. Geol.* **513**, 239–249 (2019).
27. Rouxel, O., Ludden, J., Carignan, J., Marin, L. & Fouquet, Y. Natural variations of Se isotopic composition determined by hydride generation multiple collector inductively coupled plasma mass spectrometry. *Geochim. Cosmochim. Acta* **66**, 3191–3199 (2002).
28. Scott, E. R. D. & Krot, A. N. in *Treatise on Geochemistry* 2nd edn (eds Holland, H. D. & Turekian, K. K.) 65–137 (Elsevier, 2014).
29. Labidi, J., Cartigny, P. & Moreira, M. Non-chondritic sulphur isotope composition of the terrestrial mantle. *Nature* **501**, 208–211 (2013).
30. Suer, T.-A., Siebert, J., Remusat, L., Menguy, N. & Fiquet, G. A sulfur-poor terrestrial core inferred from metal–silicate partitioning experiments. *Earth Planet. Sci. Lett.* **469**, 84–97 (2017).
31. Palme, H. & O'Neill, H. S. C. in *Treatise on Geochemistry* 2nd edn (eds Holland, H. D. & Turekian, K. K.) 1–39 (Elsevier, 2014).
32. Righter, K., Humayun, M. & Danielson, L. Partitioning of palladium at high pressures and temperatures during core formation. *Nat. Geosci.* **1**, 321–323 (2008).
33. Fischer-Gödde, M. & Becker, H. Osmium isotope and highly siderophile element constraints on ages and nature of meteoritic components in ancient lunar impact rocks. *Geochim. Cosmochim. Acta* **77**, 135–156 (2012).
34. Hopp, T. & Kleine, T. Nature of late accretion to Earth inferred from mass-dependent Ru isotopic compositions of chondrites and mantle peridotites. *Earth Planet. Sci. Lett.* **494**, 50–59 (2018).
35. Creech, J. B. et al. Late accretion history of the terrestrial planets inferred from platinum stable isotopes. *Geochem. Perspect. Lett.* **3**, 94–104 (2017).
36. Creech, J. B., Moynier, F. & Bizzarro, M. Tracing metal–silicate segregation and late veneer in the Earth and the ureilite parent body with palladium stable isotopes. *Geochim. Cosmochim. Acta* **216**, 28–41 (2017).
37. Fischer-Gödde, M. et al. Ruthenium isotope constraints on the timing of volatile element accretion. *Goldschmidt Abstr.* **2018**, 722 (2018).
38. Day, J. M. D., Walker, R. J. & Warren, J. M. ¹⁸⁶Os–¹⁸⁷Os and highly siderophile element abundance systematics of the mantle revealed by abyssal peridotites and Os-rich alloys. *Geochim. Cosmochim. Acta* **200**, 232–254 (2017).
39. Dasgupta, R., Chi, H., Shimizu, N., Buono, A. S. & Walker, D. Carbon solution and partitioning between metallic and silicate melts in a shallow magma ocean: implications for the origin and distribution of terrestrial carbon. *Geochim. Cosmochim. Acta* **102**, 191–212 (2013).
40. Schönbächler, M., Carlson, R. W., Horan, M. F., Mock, T. D. & Hauri, E. H. Heterogeneous accretion and the moderately volatile element budget of Earth. *Science* **328**, 884–887 (2010).
41. Bergin, E. A., Blake, G. A., Ciesla, F., Hirschmann, M. M. & Li, J. Tracing the ingredients for a habitable earth from interstellar space through planet formation. *Proc. Natl Acad. Sci. USA* **112**, 8965–8970 (2015).
42. Carignan, J. & Wen, H. Scaling NIST SRM 3149 for Se isotope analysis and isotopic variations of natural samples. *Chem. Geol.* **242**, 347–350 (2007).

Author contributions

S.K. designed the project, J.-P.L. provided the samples and their relevant petrogenetic features, M.I.V.-R. prepared the samples and performed the Se isotope analysis and, together with S.K. and A.Y., interpreted the data and wrote the manuscript with contributions from all the authors.

Competing interests

The authors declare no competing interests.

Additional information

Supplementary information is available for this paper at https://doi.org/10.1038/s41561-019-0414-7.

Reprints and permissions information is available at www.nature.com/reprints.

Correspondence and requests for materials should be addressed to M.I.V.

Publisher's note: Springer Nature remains neutral with regard to jurisdictional claims in published maps and institutional affiliations.

Methods

Most of the samples analysed in this work were received as fine powder materials, except for sample 15-EDL/007, which was cut by a rock saw into smaller pieces that were then crushed and finally pulverised using an agate disk mill. Analytical procedures are described in detail in Yierpan et al.[20] and Kurzawa et al.[21], and only a brief summary of the most important aspects is given here.

Between 100 and 500 mg of sample powders were weighed in perfluoroalkoxy alkane beakers together with proportional amounts of ^{77}Se–^{74}Se double spike solutions to ensure sample–spike equilibration during digestion. Samples were then digested following the hotplate HF–HNO$_3$ routine procedure described in Yierpan et al.[20]. Spinel grains were visible in some peridotites after digestion. However, orthopyroxene, clinopyroxene and spinel in peridotites do not contain detectable amounts of Se (ref. [43]) and instead, this element is considered to be mainly hosted in base metal sulfides and platinum group minerals[22,43]. Moreover, several studies in which mantle rocks were digested with inverse aqua regia in a high-pressure asher (HPA-S), a procedure that ensures the complete dissolution of spinel grains, report whole-rock Se concentrations similar to those obtained by HF–HNO$_3$ digestion[5,20,44]. However, to evaluate the possible effects of an incomplete dissolution of spinel in the Se isotope composition of peridotites, independent digestions in two peridotite samples (FONB-93 and DR33) were carried out with an Anton Paar HPA-S. For this, 1 g of sample powder together with adequate amounts of Se double spike were digested with 7.5 ml of inverse aqua regia (14.5 M HNO$_3$ and 10.5 M HCl, 3:1 molar ratio) in quartz glass vessels at 220 °C and 100 bar for 16 h. After digestion, samples were dried down at 65 °C and were subsequently treated as those digested with HF–HNO$_3$ to ensure complete digestion and desilicification. Se was separated from the sample matrix using Eichrom AG1-X8 (100–200 mesh) and AG 50W-X8 (100–200 mesh) anion and cation exchange resins, respectively, following the protocol described in Yierpan et al.[20].

After separation, samples were dissolved in 1 ml of 2 M HCl for analyses on a ThermoFisher Scientific Neptune Plus MC–ICP–MS coupled with a CETAC HGX-200 hydride generator. The Se concentration and isotope composition were measured simultaneously using the operating conditions, data acquisition and reduction procedures described in detail in Kurzawa et al.[21]. Measurements were performed in low-resolution mode, with a sample uptake rate of 0.181 ml min^{-1}. Each analysis included 40 cycles with an integration time of 4.194 s. An analytical sequence generally consisted of the measurement of a double spike NIST SRM 3149 reference standard before and after each sample, and a double spike MH-495 reference standard analysed at the beginning, the end and in the middle of the sequence. Standard solutions and, when possible, samples were prepared to have matched concentrations of ~30 ng ml^{-1}; under these conditions, the typical sensitivity of the instrument was ~ 900 mV on ^{82}Se using a 10^{11} Ω amplifier. Backgrounds were measured before each sample (and standard) analysis using pure 2 M HCl and were used for on-peak zero corrections.

The long-term analytical reproducibility of Se isotope measurements is 0.07‰ based on repeated analyses of the inter-laboratory standard MH-495. These analyses were done for 30 ng ml^{-1} Se solutions and include those previously reported by Yierpan et al.[20] and those performed during this study, and together they yield an average $\delta^{82/76}$Se value of $-3.25 \pm 0.07‰$ (2 s.d., $n = 101$, Supplementary Table 3). This is in agreement with a previously reported value of $-3.27 \pm 0.13‰$ (2 s.d., $n = 10$) on 15 ng ml^{-1} Se solutions[21] and is within the range of literature data[42,45,46]. In addition, the analytical reproducibility of Se isotope measurements in peridotites was evaluated by repeated analyses of samples FONB 93 ($n = 5$) and TUR7 ($n = 6$), which yield a 2 s.d. of 0.10‰ (Supplementary Table 2). In terms of accuracy, our average $\delta^{82/76}$Se of the US Geological Survey reference material BHVO-2 ($0.15 \pm 0.10‰$, $n = 4$) agrees well with data reported by Yierpan et al.[20] using an HF–HNO$_3$ ($0.18 \pm 0.10‰$) or an HPA-S digestion ($0.22 \pm 0.10‰$ with ~75% Se extraction). Further discussion of our reproducibility and accuracy of measurements is given in the Supplementary Information.

Each sample was individually digested and analysed 2–6 times in different analytical sessions. Particular care was taken with very depleted samples, such as harzburgite 64-3, whose digestions (up to six) had to be combined into one before being analysed to ensure the minimum amount of Se required for precise isotope measurements (~5 ng) (ref. [21]). Our peridotite dataset is thus composed of 51 digestions and 32 measurements over different analytical sessions. Generally, ~30 ng of Se were analysed for fertile lherzolites, whereas for depleted peridotites, the amount of Se analysed ranged between 7 and 30 ng depending on their concentrations (Supplementary Table 2). Prior to each analytical session, samples were checked for possible arbitrarily remaining germanium (Ge) that would

contribute interferences. Usually, Ge signals were lower than background levels. However, if higher, 1 ml of 10.5 M HCl was added to the sample and subsequently dried down at 90 °C (ref. [20]). This procedure allows for the complete elimination of Ge and, although it results in minor Se losses for rock matrices (~10–30% in the case of peridotites), any associated isotopic fractionation is corrected by the use of the double spike technique[21]. Other possible polyatomic interferences on the measured Se isotope masses were suppressed by admixing methane throughout the entire measurement session, which also allowed for an enhancement of the Se signal[21]. The $\delta^{82/76}$Se value of each sample (and MH-495 standard), obtained after double spike deconvolution, was normalized by the average $\delta^{82/76}$Se of the NIST SRM 3149 standard measured immediately before and after the sample. As published Se concentrations exist for most of the samples analysed in this study[5,16,22,44,47] (Supplementary Table 2), an almost exact spike-to-sample ratio was adjusted without pre-concentration measurements. In the few cases in which Se concentrations were unknown, samples were first analysed with an iCAP-Qc ICP–MS, as described below.

A ThermoFisher Scientific iCAP-Qc ICP–MS coupled with an ESI hydrideICP hydride generation system was used for pre-concentration Se measurements. The analytical procedure is described in detail in Yierpan et al.[20]. Setting parameters were tuned daily by using ~0.5 ng g^{-1} Se of unspiked NIST SRM 3149 standard solution, and measurements were performed in the Icap-Qc STD mode for highest sensitivity. The ^{77}Se and ^{78}Se isotopes were monitored with a dwell time of 0.03 s. Samples were prepared to have matched concentrations with the standard and, under typical operating conditions, the standard solution yielded intensities of ~30,000 counts per second on ^{78}Se. Each analytical session included four standard solutions, three measured at the beginning and one at the end of the session. Backgrounds were measured before each sample and standard analysis using pure 2 M HCl and were then subtracted from their analysed peak intensities, followed by correction of the instrumental mass bias using the natural ^{77}Se/^{78}Se ratio. Counts for Se were based on ~400 measurements per sample after signal stabilization and thereafter converted into concentrations (ng g^{-1}).

Total analytical blanks, which were processed using the same procedure as outlined above for the samples, were indistinguishable from background intensities (equivalent to ~0.05 ng ml^{-1} Se; ref. [17]) during the analysis, and the recovery yield of Se, including sample dissolution, ion exchange chemistry and hydride generation efficiency, ranged between ~60 and 95%. Regarding the use of different digestion techniques, the Se concentrations and $\delta^{82/76}$Se values of samples FONB-93 and DR33 by HPA-S are indistinguishable, within error, to those obtained using HF–HNO$_3$ digestion, and thus they are considered in the average concentrations and isotopic values of each sample (Supplementary Table 2). The Se concentration and isotopic signature of peridotites are independent of the digestion technique used here, which confirms earlier observations on the Se isotope composition of basalts[20].

Data availability

The data that support the findings of this study are provided as Supplementary Tables 1–7.

References

43. König, S., Lissner, M., Lorand, J.-P., Bragagni, A. & Luguet, A. Mineralogical control of selenium, tellurium and highly siderophile elements in the Earth's mantle: evidence from mineral separates of ultra-depleted mantle residues. *Chem. Geol.* **396**, 16–24 (2015).

44. König, S., Luguet, A., Lorand, J.-P., Wombacher, F. & Lissner, M. Selenium and tellurium systematics of the Earth's mantle from high precision analyses of ultra-depleted orogenic peridotites. *Geochim. Cosmochim. Acta* **86**, 354–366 (2012).

45. Vollstaedt, H., Mezger, K. & Leya, I. The isotope composition of selenium in chondrites constrains the depletion mechanism of volatile elements in Solar System materials. *Earth Planet. Sci. Lett.* **450**, 372–380 (2016).

46. Zhu, J.-M., Johnson, T. M., Clark, S. K. & Xiang-Kun, Z. High precision measurement of selenium isotopic composition by hydride generation multiple collector inductively coupled plasma mass spectrometry with a ^{74}Se–^{77}Se double spike. *Chin. J. Anal. Chem.* **36**, 1385–1390 (2008).

47. Lorand, J.-P., Luguet, A., Alard, O., Bezos, A. & Meisel, T. Abundance and distribution of platinum-group elements in orogenic lherzolites; a case study in a Fontete Rouge lherzolite (French Pyrénées). *Chem. Geol.* **248**, 174–194 (2008).